

Low energy elastic scattering of H, D and T on ^3He and ^4He

B.J.P. Jones^{1, 2, *}

¹*Department of Physics, University of Texas at Arlington, Arlington, TX 76019, USA*

²*Department of Physics and Astronomy, University of Manchester, Oxford Road, Manchester, M13 9PY, UK*

(Dated: February 2, 2026)

Motivated by the needs of atomic tritium sources for neutrino mass experiments, we present calculations of energy-dependent elastic scattering cross sections of hydrogen isotopes (H, D and T) on helium isotopes (^3He and ^4He) in the temperature range 1 mK to 300 K. The tritium-on-helium cross sections are found to be enhanced over their hydrogen-on-helium counterparts by a near-threshold resonant s-wave bound state at low energy, similar to that predicted in the triplet T-T system. While the energy-dependent cross sections span a wide range at low energy due to this s-wave enhancement, they tend toward a common value at high energy where the scattering becomes effectively geometric in nature.

I. INTRODUCTION

The low energy elastic scattering of hydrogen-like atoms on each other and on isotopes of helium is of interest in a variety of contexts in atomic physics. In particular, the dynamics of cold atomic tritium are receiving continuing attention in the context of experiments that aim to measure the mass of the neutrino [1] using atomic (T) rather than molecular (T_2) sources [2]. To use T for this purpose, molecular tritium must be dissociated [3, 4] and then cooled to the point where it can be stored magnetically, which is feasible at temperatures of at most a few tens of milikelvin. The vapor properties, evaporative cooling efficiency and loss rates of tritium atoms in proposed cooling systems and magnetic traps depends strongly on their elastic and inelastic scattering cross sections [5], which are as-yet unmeasured.

To facilitate the designs of atomic T cooling systems for proposed neutrino mass experiments including Project 8 [6], KATRIN++ [7] and QTNU [8], we recently produced a new suite of calculations of H-H and T-T scattering in all elastic and inelastic channels as a function of magnetic field and temperature [9]. These predictions enable advances in the quantitative design and optimization of properties of atomic tritium cooling systems [5].

This paper presents a suite of follow-up calculations for a second set of relevant processes, obtained using a subset of the methods of Ref [9]. These are the cross sections of atomic hydrogen isotopes scattering from helium atoms. While less central to experiment design than their T-T scattering counterparts, tritium-helium scattering informs the designs of atomic tritium sources for neutrino physics in at least the following contexts:

1. The decay of T to ^3He occurs continuously within an atomic T source, and hence trace levels of ^3He are both initially present in incoming T_2 gas and produced continuously within trapped T vapor. Since ^3He is not itself magnetically trapped it will

ultimately be either turbo- or cryo-pumped from the active volume. Nevertheless, a stable background level of ^3He is expected in the tritium cell, leading to ^3He -T scattering, which should be accounted for when modeling tritium vapor dynamics. The low energy elastic scattering cross section of T on ^3He has not been previously reported.

2. Slowing of tritium on cryogenic buffer gas [10] has been discussed as a possible way to partially slow and cool atomic T. As the lightest gases which have no chemical activity, ^3He and ^4He are natural choices for this purpose. The slowing and cooling rates are determined by the energy dependent ^3He -T and ^4He -T cross sections.
3. Supersonic expansion sources have been proposed to produce cold beams of H and T by energy transfer of the atoms to expanding jets of helium [8]. The detailed dynamics depend on energy transfer to the expansion gas via H-He and T-He scattering. In particular, the relative efficacy of the system for the projected T application based on more easily studied H test systems depends on the ratio of these cross sections.
4. Cryogenic dissociation sources have been recently proposed [11], whose behavior is governed in part by the interaction of T with helium isotopes. In the study of Ref. [11], helium-helium cross sections were used as placeholders for tritium-helium values. Since the electronic structure of T and He are different, the quality of this approximation should be scrutinized.

The above cases motivate the present work, which provides not only tritium-helium scattering cross section predictions, but also those for all hydrogen isotopes on both helium isotopes.

II. FORMALISM AND POTENTIALS

Because neither ^3He nor ^4He have any net electronic spin, it is notable that the scattering system consid-

* ben.jones@uta.edu

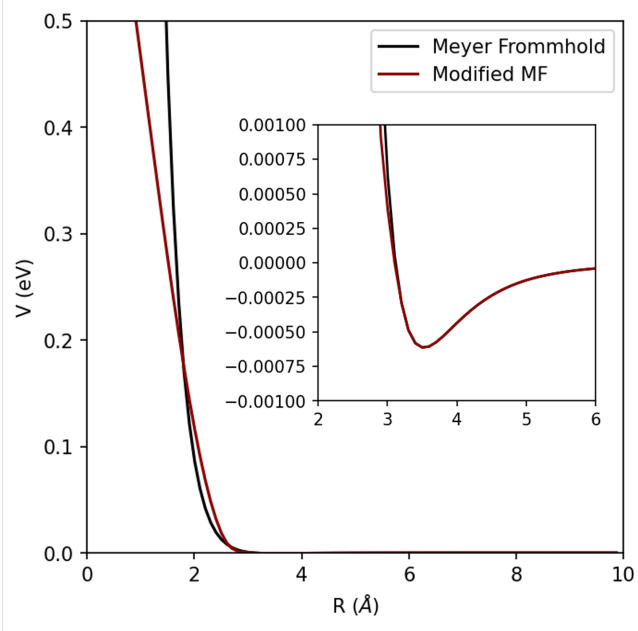


FIG. 1. Potentials used in this work. The Meyer Frommhold potential is digitized from Ref. [12], and the Modified MF potential includes the hard core modification proposed in Ref. [13].

ered here is considerably simpler than the T-T system of Ref [9]. ${}^3\text{He}$ has a nuclear spin, but the interaction of nuclear spins is very weak compared with electronic spins due to the relative size of the electronic and nuclear magnetons. As such, the rate of inelastic / spin-changing interactions in the processes discussed here is negligible. The only relevant process is thus elastic scattering. Furthermore, because the two particles involved in scattering are non-identical, no exchange symmetry considerations must be accounted for. The elastic scattering cross section depends on center-of-mass energy, reduced mass and inter-atom potential, but not on applied magnetic field, and can be obtained via a partial-wave phase-shift analysis.

Following the approach outlined in Ref [9], and similar to that employed in Ref. [14] for H-H elastic scattering and [15] for T-T elastic scattering, we solve the one-dimensional Schrodinger equation for nuclear motion under the Born Oppenheimer approximation. The relevant potential $V(R)$ is the ground state electron energy derived by solving for the three-electron ground state at fixed nuclear separation R , which is then used to model dynamical evolution of a nuclear coordinate wave function, $\psi(R)$.

Through axial symmetry only $m=0$ partial waves are relevant to the nuclear motion, and the radial wave function $u_{El}(R)$ for each orbital angular momentum l and

energy E satisfies the central Schrodinger equation,

$$\left\{ \frac{d}{dR^2} + \frac{2\mu}{\hbar} \left[E - V(R) - \frac{l(l+1)\hbar^2}{2\mu R^2} \right] \right\} u_{El}(R) = 0, \quad (1)$$

with μ the reduced mass and \hbar Planck's constant. The large-distance solution at $R \rightarrow \infty$ is expressed in terms of partial wave phase shifts δ_l as

$$\lim_{R \rightarrow \infty} \psi(\mathbf{R}) = e^{ikR} + \frac{e^{ikR}}{R} f(\theta, \phi), \quad (2)$$

$$f(\theta) = \sum_{l=0}^{\infty} (2l+1) \frac{e^{(2i\delta_l(E)-1)}}{2ik} P_l(\cos(\theta)). \quad (3)$$

where k is the wave vector. The cross section can then be obtained from these phase shifts as

$$\sigma = \int d\Omega |f(\theta, \phi)|^2 = \frac{4\pi}{k^2} \sum_l (2l+1) \sin^2 [\delta_l(E)]. \quad (4)$$

Eq 4 differs from the similar equation in of Ref. [9] via 1) its pre-factor of 4 rather than 8, and 2) and a sum over both odd and even values of l rather than even-only, both of these adjustments deriving from the fact we are now handling scattering of distinguishable atoms rather than indistinguishable bosons.

At low energy, the cross section is determined by the s-wave scattering length alone, per

$$\sigma = 4\pi a_s^2, \quad (5)$$

which is obtained from the low energy limit of the s-wave phase shift $\delta_0(k)$ as

$$a_s = - \lim_{k \rightarrow 0} \frac{\tan(\delta_0(k))}{k}. \quad (6)$$

All of the phase shifts are in practice found by solving Eq. 1 outward from low R , and comparing the phase of the outgoing spherical wave at long-distance against the free-particle solution of the same energy that is non-singular at the origin. This approach follows widely used methods in quantum scattering theory. [16]

To obtain scattering cross sections from Eq. 1 we require the appropriate scattering potential. In Ref. [12], Meyer and Frommhold calculated the interaction potential as a function of atomic separation in the He-He system using a multi-reference configuration interaction method. The Meyer Frommhold potential is shown in Fig. 1. Using the Meyer Frommhold potential, In Ref [13] Chung and Dalgarno calculated the diffusion constants for hydrogen in helium and helium in hydrogen. Comparison to experimental results at standard temperature and pressure showed a 15% discrepancy, leading the authors to consider a modified potential with a steeper repulsive core to better match these data. The modified Meyer Frommhold potential is shown overlaid in Fig. 1. Here we compare predictions made using both modified and

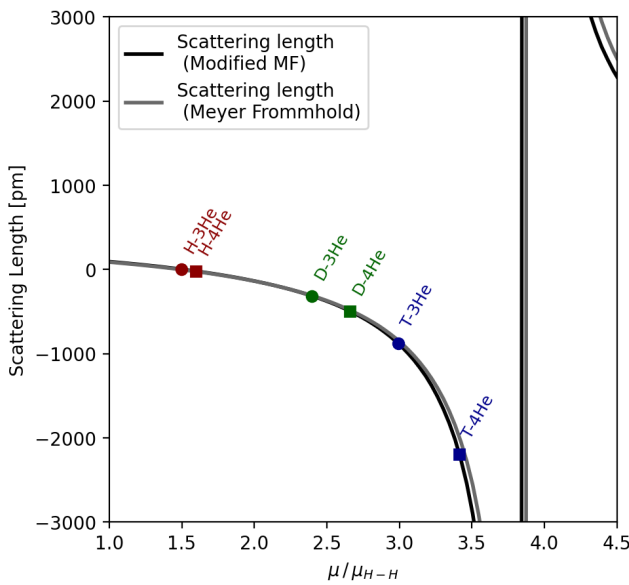


FIG. 2. Reduced mass dependent s-wave scattering length a_s for the H-He system as a function of reduced mass μ in units of the H-H reduced mass μ_{H-H} . The low energy scattering lengths for the various isotope combinations of interest are indicated on the curve and reported in Table I

un-modified Meyer Frommhold potentials. The steep inner core is found to be most relevant for the lighter combinations at the lowest energies, but will be shown to be marginal over most of the parameter space considered for T-He scattering.

III. RESULTS

We first calculate the low energy limit of the scattering cross section, which depends only on the s-wave scattering length via Eq. 6. Since there are no non-trivial spin or magnetic-field dependencies, all of the (H,D,T) on (^3He , ^4He) scattering cross sections at $k \rightarrow 0$ can be represented as a universal function of the reduced mass μ used in solution of Eq. 1. Fig 2 shows the predicted s-wave scattering length as a function of μ with the experimentally relevant values marked, where the reduced masses are reported relative to the H-H scattering system $\mu_{H-H} = 8.3401 \times 10^{-28}$ kg. Table I provides the value of μ , the s-wave scattering length, and low-temperature cross section for each two-body processes. Using the modified Meyer Frommhold potential, Chung and Dalgarno reported an s-wave scattering length of $a_s = 0.359$ Bohr for H- ^4He , which compares favorably against our calculated value, which is $a_s = 0.360$ Bohr, in these units. This agreement provides a useful validation of our methodology and implementation.

For the majority of the atom pairs considered, the modified and unmodified Meyer Frommhold potentials provide comparable predictions, predicting a similar scat-

Process	μ / μ_{H-H}	a_s (mod-MF) [pm]	a_s (MF) [pm]
H- ^3He	1.499	3.85	-0.69
H- ^4He	1.598	-19.1	-12.1
D- ^3He	2.396	-312	-309
D- ^4He	2.658	-493	-481
T- ^3He	2.993	-880	-842
T- ^4He	3.414	-2200	-1990

TABLE I. Zero energy limit of the s-wave scattering lengths for each isotope combination calculated using the modified Meyer Frommhold (left) and original Meyer Frommhold (right) potentials. The low energy limit of the scattering cross section can be obtained from Eq. 6.

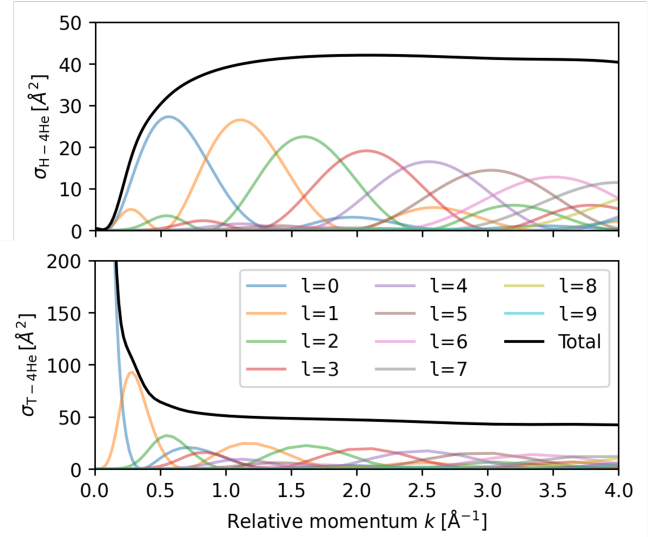


FIG. 3. Partial wave components of the scattering cross sections for the H- ^4He (top) and T- ^4He (bottom) processes. The results are similar over most relative momentum values, with the exception of the resonantly enhanced s-wave amplitude at low energy, as shown on Fig. 2.

tering length to within a few percent. The exception is the $^3\text{He}-\text{H}$ process, which happens to be close in reduced mass to where the scattering length vs μ curve crosses $a_s = 0$ in Fig. 2. Where they are discrepant, the modified Meyer Frommhold potential is likely to be more reliable since it matches experimental data on hydrogen diffusion in helium [13]. Nevertheless, it is cautioned that an accurate prediction of the low energy $^3\text{He}-\text{H}$ cross section in particular would benefit from development of more precise ab-initio potentials. For all other channels, the potentials appear sufficiently robust to make a confident prediction at the few-percent level.

Because the potential is attractive at long distances, bound states can be supported as long as the atomic masses are sufficiently large to stabilize the Van Der Waals molecule. The clear pole in Fig. 2 shows that the first bound state is introduced (*i.e.*, becomes present with energy $E \sim 0$) for reduced masses of $\sim 3.9 \mu_{H-H}$. This is higher in mass than the threshold for the similar bound

state that was found to occur in the scattering of two hydrogen-like atoms, which appeared at $\sim 3.2 \mu_{H-H}$ [9]. The difference between these thresholds owes to the difference between shapes of the Meyer Frommhold and Silvera Triplet [17] potentials. Nevertheless, just as in the hydrogen-hydrogen scattering system, this near-resonant bound state leads to enhancements of the cross sections for heavier isotope combinations, with both T-³He and T-⁴He scattering being significantly stronger than the corresponding H-³He and H-⁴He scattering processes. As in T-T scattering, the enhancement factors are of order 10² in scattering length, corresponding to order 10⁴ in cross section.

To calculate energy dependent cross sections we require the phase shifts at non-zero energy and also the higher partial wave contributions. Fig. 3 shows the partial wave decomposition of the H-⁴He and T-⁴He processes for the energy-dependent calculation. The major difference in the shapes of these cross sections is seen to emerge from the varying amounts of s-wave enhancement, as discussed above. At higher energy, the higher partial waves superpose to provide a constant cross section that becomes independent of energy for hard collisions. This is the geometric limit, where the process becomes an effectively hard-sphere scatter with the cross section determined by the atomic Van Der Waals radii.

Fig. 4 shows the predicted energy-dependent cross sections for each of the isotope pairs, and is the primary result of this work. As previously observed, the low energy cross sections are dictated by the s-wave scattering length enhancement with a strong dependence on reduced mass of the colliding pair. The high energy cross sections converge to a common limiting value, as expected given the equivalent electronic structure in each case. It is notable that this limit is consistent the expected high energy hard-sphere scattering cross section of $\sigma = 2\pi r^2$ (including the factor of 2 for shadowing in quantum scattering [18]) with r given the summed Van Der Waals radii of hydrogen ($r_H = 100$ pm) and helium ($r_{He} = 140$ pm). This “black-disk limit” reference point is marked with a cross at the high energy side of Fig. 4.

The differences between the Meyer Frommhold and Modified potentials are marginal at high energy, becoming more substantial for soft collisions and for lighter atoms. The Modified potential is taken as our primary prediction since it provides agreement with diffusion data [13]. The effect of the core modification is indicated via the shaded bands in Fig 4. For all heavier isotope combinations this effect is small over the full energy range. For H-³He scattering, the cross section below ≤ 100 mK involves an especially small s-wave phase shift, and begins to depend more strongly on the details of this core treatment, as observed above.

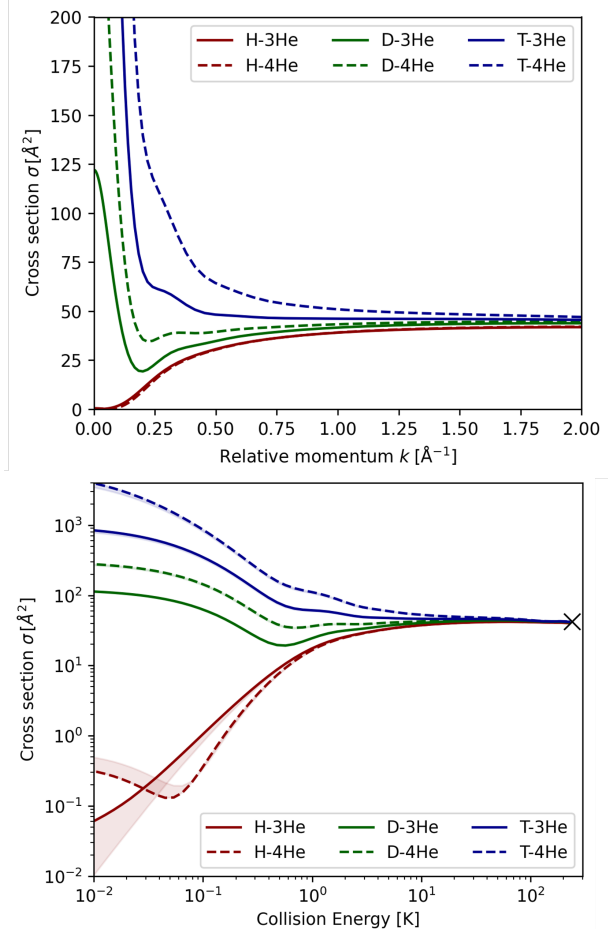


FIG. 4. Momentum-dependent (top) and energy-dependent (bottom) cross section for each of the processes considered in this paper. The energy reported is the center of mass collision energy in units of Kelvin, $p^2/(2\mu k_B)$. The black X shows the hard-sphere cross prediction based on the Van Der Waals radii of hydrogen and helium. The shaded bands show the difference between the Modified and Unmodified Meyer Frommhold potentials.

IV. CONCLUSION

We have reported calculations of the elastic scattering cross sections of H, D, and T on ³He and ⁴He. Although considerably simpler than the calculations of T-T cross sections presented in Ref. [9] due to the lack of spin-spin interactions, most of the presented cross sections have not been previously reported in the literature. Their values are required to inform aspects of the design and development of atomic sources for neutrino mass experiments. We find that the tritium-on-helium scattering cross sections exhibit a similar resonant enhancement to tritium-on-tritium triplet elastic scattering, albeit with a different resonance threshold in reduced mass, owing to the differently shaped interaction potential. The energy dependent cross sections are presented for all processes, and show a wide spread of values at low energy

due to mass dependent enhancement of the s-wave contribution, but convergence to a common value that is consistent with the black disc limit at energies above a few tens of Kelvin. The complete energy-dependent cross sections are supplied as tables in the supplementary information [19], and an open-source code is provided for reproducing these results [20].

ACKNOWLEDGEMENTS

BJPJ is supported by the US Department of Energy under awards DE-SC0024434 and DE-SC0019223, and

the Gordon and Betty Moore Foundation, grant DOI 10.37807/GBMF13782. We thank Sergey Vasiliev for pointing out the need for T-He cross sections for cryogenic discharge sources and fruitful discussions, as well as Morgan Elliott and Paul Harmston for useful feedback during the development of these calculations. Finally we thank the Project 8 and QTNM collaborations for providing the motivation for our wider program of low-energy tritium cross section evaluations.

[1] J. A. Formaggio, A. L. C. de Gouv  a, and R. H. Robertson, Direct measurements of neutrino mass, *Physics Reports* **914**, 1 (2021).

[2] W. C. Pettus, the Project 8 Collaboration, *et al.*, Overview of project 8 and progress towards tritium operation, in *Journal of Physics: Conference Series*, Vol. 1342 (IOP Publishing, 2020) p. 012040.

[3] C. Outten, J. Barbour, and W. Wampler, Characterization of electron cyclotron resonance hydrogen plasmas, *Journal of Vacuum Science & Technology A: Vacuum, Surfaces, and Films* **9**, 717 (1991).

[4] K. Tschersich and V. Von Bonin, Formation of an atomic hydrogen beam by a hot capillary, *Journal of applied physics* **84**, 4065 (1998).

[5] A. A. Esfahani, S. Bhagvati, S. B  ser, M. Brandsema, R. Cabral, V. Chirayath, C. Claessens, N. Coward, L. de Viveiros, P. Doe, *et al.*, Dynamics of Magnetic Evaporative Beamline Cooling for Preparation of Cold Atomic Beams, arXiv preprint arXiv:2502.00188 (2025).

[6] A. Ashtari Esfahani, S. B  ser, N. Buzinsky, M. Carmona-Benitez, C. Claessens, L. De Viveiros, P. Doe, M. Fertl, J. Formaggio, J. Gaison, *et al.*, Tritium beta spectrum measurement and neutrino mass limit from cyclotron radiation emission spectroscopy, *Physical review letters* **131**, 102502 (2023).

[7] N. Kovac, F. Adam, B. Bornschein, W. Gil, F. Gl  ck, S. Heyns, S. Kempf, A. Kopmann, M. M  ller, R. Sack, *et al.*, Katrin++-development of new detector technologies for a future neutrino mass experiment with tritium, in *DPG-Fr  hjahrstagung der Sektion Materie und Kosmos (SMuK 2025), G  ttingen, Deutschland, 31.03.2025-04.04.2025* (2025).

[8] A. A. Amad, F. Deppisch, M. Fleck, J. C. Gallop, T. Goffrey, L. Hao, N. Higginbotham, S. D. Hogan, S. B. Jones, L. Li, *et al.*, Determining absolute neutrino mass using quantum technologies, *New Journal of Physics* (2025).

[9] M. G. Elliott and B. J. P. Jones, Elastic and spin-changing cross sections of spin-polarized atomic tritium, *Phys. Rev. A* **112**, 062818 (2025).

[10] N. R. Hutzler, H.-I. Lu, and J. M. Doyle, The buffer gas beam: An intense, cold, and slow source for atoms and molecules, *Chemical reviews* **112**, 4803 (2012).

[11] A. Semakin, J. Ahokas, T. Kiilerich, S. Vasiliev, F. Nez, P. Yzombard, V. Nesvizhevsky, E. Widmann, P. Crivelli, C. Rodenbeck, *et al.*, Cryogenic source of atomic tritium for precision spectroscopy and neutrino-mass measurements, arXiv preprint arXiv:2511.08313 (2025).

[12] W. Meyer and L. Frommhold, Long-range interactions in h-he: ab initio potential, hyperfine pressure shift and collision-induced absorption in the infrared, *Theoretica chimica acta* **88**, 201 (1994).

[13] H. Chung and A. Dalgarno, Diffusion of hydrogen atoms in helium gas and helium atoms in hydrogen gas, *Physical Review A* **66**, 012712 (2002).

[14] B.R.Joudeh, Scattering Properties of Ground-State Spin-Polarized Atomic Hydrogen, *Physica B* , 41 (2013).

[15] A. F. Al-Maaitah, Scattering Properties of Spin-Polarized Atomic Tritium, *European Scientific Journal* **8**, 170 (2012).

[16] S. Weinberg, *Lectures on Quantum Mechanics* (Cambridge University Press, 2015).

[17] I. F. Silvera and J. Walraven, *Spin-Polarized Atomic Hydrogen*, edited by D. F. Brewer, *Progress in Low Temperature Physics*, Vol. X (Elsevier Science Publishers B.V., 1986).

[18] J. J. Sakurai and J. Napolitano, *Modern quantum mechanics* (Cambridge University Press, 2020).

[19] B.J.P. Jones, H-He cross section data tables (2026), https://github.com/UTA-NURES/AtomicTrit/blob/HeH/examples/Tables/HeH_CrossSections.csv.

[20] B.J.P. Jones, Atomic tritium calculator, Helium branch (2026), <https://github.com/UTA-NURES/AtomicTrit/>.